Journal of Zhejiang University-SCIENCE A (Applied Physics & Engineering)
ISSN 1673-565X (Print); ISSN 1862-1775 (Online)
www.jzus.zju.edu.cn; www.springerlink.com
E-mail: jzus@zju.edu.cn

Experimental investigation on flame stabilization of a kerosene-fueled scramjet combustor with pilot hydrogen*

Wen SHI, Ye TIAN†‡, Wan-zhou ZHANG, Wei-xin DENG, Fu-yu ZHONG, Jia-ling LE

China Aerodynamic Research and Development Center, Mianyang 621000, China

†E-mail: tianye@cardc.cn

Received Nov. 18, 2019; Revision accepted Apr. 1, 2020; Crosschecked July 15, 2020

Abstract: Flame stabilization in a kerosene-fueled scramjet combustor was investigated experimentally through Schlieren, flame luminosity, and wall pressure measurement, aiming to obtain better insight into combustion characteristics. Experiments were conducted in a direct-connected supersonic combustion facility with inflow conditions of Mach number 2.0, stagnation pressure 0.82 MPa, and temperature 950 K, simulating the flight condition of Mach number 4.0. Results revealed that kerosene was able to be ignited when the equivalence ratio of pilot hydrogen reached 0.080, but was unsuccessful when the equivalence ratio was 0.040. Once ignited, the intense combustion induced high back pressure forcing the flame to spread into the isolator. The pilot flame invariably appeared in the cavity shear layer and attached to the cavity ramp under different equivalence ratios of pilot hydrogen. With the mass flux of pilot hydrogen increased, the kerosene flame located near the cavity ramp was asymmetrical and unstable since it propagated upstream repeatedly. Therefore, the kerosene could be ignited by a suitable equivalence ratio of continuous pilot hydrogen, potentially accompanied with unstable combustion.

Key words: Scramjet; Flame stabilization; Pilot hydrogen; Kerosene; Supersonic combustion
https://doi.org/10.1631/jzus.A1900565 **CLC number:** V43

1 Introduction

Combustion characteristics, which contain mixing (Huang and Yan, 2013; Huang et al., 2016), ignition, flame stabilization (Liao et al., 2018), and oscillation in scramjet combustors, are still not fully comprehended despite nearly seven decades of research. It is the inability of measuring crucial flow properties experimentally that leads to this situation. Along with the improvement of measurement, large numbers of experiments have been carried out to better understand the combustion characteristics and contributory factors.

Chang JT et al. (2018) and Zhang et al. (2018) investigated combustion stabilization in a kerosene-fueled combustor, equipped with a strut, experimentally and numerically. A large mass flux of fuel was injected perpendicularly to the side walls. The fuel was ignited by a pilot flame, which stabilized in the internal flow duct of the strut. Then a globally stable flame was established. The specific geometry of the strut and the strategy of combustion organization would lead to a thermal choking at the exit of the strut, which was propitious for self-stabilization of the pilot flame. Combustion characteristics in a wide range of equivalence ratios ranging from 0.15 to 0.75 were obtained. Self-stabilization of the flame failed when the total equivalence ratio of kerosene was larger than 0.45. Therefore, flame stabilization was sensitive to the geometry of the strut. Niioka et al. (1995) proposed a special strut, which consisted of two divided parts. Flame stabilization was studied through experiments conducted under a flow

‡ Corresponding author
* Project supported by the National Natural Science Foundation of China (No. 51706237), the China Aerodynamic Research and Development Center Fundamental and Frontier Technology Research Fund, and the Postdoctoral Research Foundation of China (No. 2019M653953)
ORCID: Ye TIAN, https://orcid.org/0000-0001-9955-3438

condition of Mach number 1.5. The pre-condition of global flame establishment was that hydrogen located between the two parts of the strut ignited. The distance between the two parts of strut had great influence on the characteristics of flame stabilization.

In order to enhance ignition reliability under extreme conditions, a gliding arc igniter applied to ignite ethylene has been designed and tested, in Mach number 2.52 supersonic flow, by Feng et al. (2018). Compared to the traditional spark plug, the gliding arc igniter was capable of enlarging the combustion area but with intermittent combustion of ethylene in the cavity. This was potentially caused by the reignition characteristic of the gliding arc igniter. Experimental results have verified the feasibility that the gliding arc plasma could be used to achieve combustion enhancement during the process of flame stabilization. When the equivalence ratio of the upstream strut was less than 0.2, the kerosene flame stabilized in the boundary-layer separation region. As the equivalence ratio increased, the intermittent back-flash phenomenon of the kerosene flame took place in the incoming flow at Mach number 3.0 and stagnation temperature 1899 K. When the equivalence ratio was 0.2, the speed of flame was around 1.3 km/s which was larger than the C-J detonation speed (Zhu et al., 2018). Combustion characteristics and performance of the scramjet engine varied with dynamic change of equivalence ratio. Numerical investigations on flame stabilization and combustion establishment in a ramjet engine-applied splitter-plate were conducted by Zhang et al. (2015). The thickness of splitter-plate affected the spatial location of ignition as a larger thickness was beneficial for enhancing mixing dynamics and achieving complete combustion.

The stagnation temperature of the incoming flow had a significant impact on flame stabilization. This was tested by Chang EWKC et al. (2018). The stagnation temperature ranged from 1270 K to 1810 K. The results showed that a stable flame was maintained inside the cavity at 1540 K, whereas no flame was established at 1270 K although ignition was achieved. Strong ignition and intermittent flames were observed at 1810 K with combustor injection. Effects of total pressure and temperature at combustor entrance on the flame stabilization with various configurations of injectors have been investigated (Wang et al., 2017; Wang and Song, 2019). Enhancement of total pressure and temperature would extend the rich blowout limits, but would decrease and increase the lean blowout limits, respectively. The blowout limit was more sensitive to the variation of total temperature. The smaller diameter the injector had, the greater performance the combustor acquired. In addition, Kim et al. (2019) studied the flameholding characteristics of an ethylene-fueled scramjet through shadowgraph and flame luminescence image. The injection location affected flame stabilization mode and combustion stability. The transverse injection would improve flue-air mixing and the flame signals have been strengthened with the increased equivalence ratio.

The flame flashback phenomenon in an ethylene-fueled scramjet combustor was discovered and studied experimentally by Sun et al. (2008, 2012), Wang HB et al. (2013), Wang ZG et al. (2015), and Zhao et al. (2019). The fuel was ignited by spark and formed an initial flame, which spread along the cavity shear layer and expanded to the main flow. Because of the complicated interaction between flow and heat release, the flame embodied three combustion modes. The most unstable mode was the cavity-assisted jet-wake stabilized mode which possibly caused intermittent blow off.

Based on a large number of experiments, flame fluctuation was discovered with a mode of thermo-acoustic type oscillation and similar to deflagration-detonation transition. The temperature fluctuation downstream of the cavity played a vital role in the quasi-periodic oscillation of combustion or flame flashing. Therefore, the influencing factors on flame stabilization included the type of igniter, the strategy of how the fuel was injected, and the combination of flameholders.

In this paper, high-speed images are taken from the side wall and bottom wall to gain flame structures to investigate the flame stabilization in a kerosene-fueled supersonic combustor, which applies pilot hydrogen to ignite kerosene and establish a global flame.

2 Experimental

2.1 Experimental facility and the combustor configuration

To simulate the flight conditions of Mach number 4.0, a direct-connected supersonic combustion

facility with a stagnation temperature of 950 K and stagnation pressure of 0.82 MPa is used. The detailed conditions of internal flow are given in Table 1.

It can be seen that the standard deviations of flow conditions are smaller than 5%. The total mass flow rate of vitiated high-enthalpy airflow at the isolator entrance is 2.68 kg/s, and the molar compositions of O_2, H_2O, and N_2 are 21%, 12%, and 67%, respectively.

The lab-scale supersonic combustor, which is made of stainless steel, is composed of two sections as shown in Fig. 1. The first section is a rectangular isolator with a cross-section of 30 mm×150 mm, and its length is 300 mm. The second section is a single-side expansion supersonic combustor with a cavity located at the exit of the isolator. The depth of cavity D is 16 mm and the length-to-depth ratio L/D is 11. The total length of the combustor is 800 mm and the expansional section of the combustor locates from 476 mm to 1070 mm. The divergence angles are 1.4°, 2.0°, 8.0°, and 15.0° relative to the bottom wall as presented in Fig. 1b. Thus, the total expansion ratio of the combustor is 2.62.

There are two kinds of injectors located 285 mm and 325 mm away from the isolator entrance. The first one is used to inject liquid kerosene at room temperature. It is injected perpendicularly to the inflow through 15 0.3-mm-diameter portholes. The second one is applied to inject gaseous pilot hydrogen through 10 1.0-mm-diameter portholes and the pilot hydrogen is ignited by two spark plugs in the cavity floor.

The historical pressure along the center line of the wall is measured by pressure transducers at an interval of 25 mm as shown in Fig. 1a. To distinguish the status of the combustion, the wall pressure located in the cavity floor near the cavity ramp (x=425 mm) is monitored. The corresponding parameters of fuel injection are listed in Table 2.

The equivalence ratios of kerosene and hydrogen are 0.173 and 0.040 in case 1, and they are 0.173 and 0.080 in case 2. There is no injection of fuel in case 3. Compared to wall pressure distribution obtained from non-reacting flow in case 3, the effects of pilot hydrogen and different equivalence ratios on the flame stabilization can be obtained.

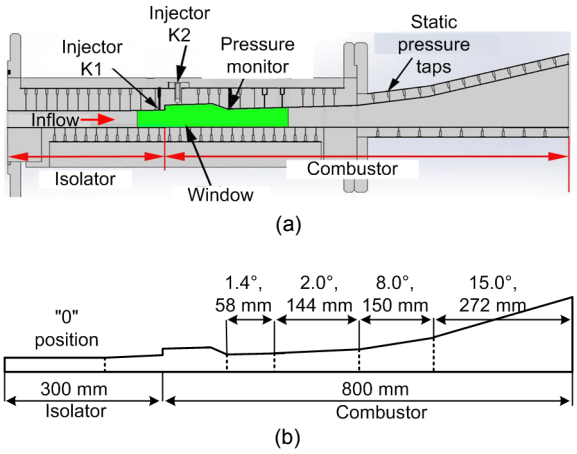

Fig. 1 Schematic illustration (a) and length description (b) of the supersonic combustor

Table 2 Fuel injection parameters of different cases

Case	Equivalence ratio	
	Hydrogen	Kerosene
1	0.040	0.173
2	0.080	0.173
3	0	0

2.2 Instrumentation

The measurements of wall pressure in the direction of stream wise are made by pressure transducers with a sampling frequency of 1 kHz, a range of 0–700 kPa, and an uncertainty of 1%. Except for the above intrusive pressure measurements, non-intrusive measuring methods including Schlieren and high-speed framing of flame luminosity have been used to investigate the development and stabilization characteristics of the flame. Schlieren images are

Table 1 Steady flow conditions of direct-connected supersonic combustion facility

Property	Location	Experimental value			Deviation, |(value−ref)/ref| (%)
		Case 1	Case 2	Case 3	
Stagnation pressure, P_t (MPa)	Nozzle entrance	0.821	0.816	0.819	0.6
Static pressure, P (MPa)	Isolator entrance	0.105	0.108	0.102	4.7
Mach number, Ma	Isolator entrance	2.011	1.982	2.020	1.4

ref indicates the design value

applied to show the evolution process of shock structure.

The images are captured by a charge-coupled device (CCD) camera. The exposure time is 1 μs and the frame rate is 10000 frames per second. The flame luminosity, which is imaged by another CCD camera with 5 nm bandwidth interference filters, is used to trace the flame zones. The exposure time is 1/2000 s. As shown in Fig. 2, Schlieren images are taken from the side wall of the combustor and the images of flame luminosity are taken from the side wall and bottom wall.

Fig. 3 shows the structure of the high-enthalpy supersonic internal flow. Upstream of the cavity step, there are several shock waves induced by the holes of the pressure transducers and fuel injection port-holes. These weak shock waves would reduce the uniformity of the internal flow, but the degree of influence is slight. The pressure argument of the 300-mm-length isolator is around 8%, which is caused by not only the boundary layer thickening but also the shock waves.

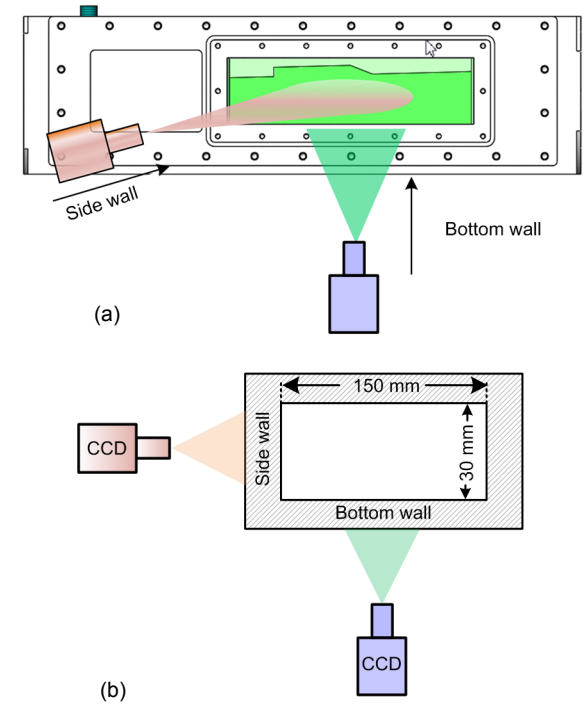

Fig. 2 Taking schematics of Schlieren image (a) and flame luminosity (b) from side wall and bottom wall

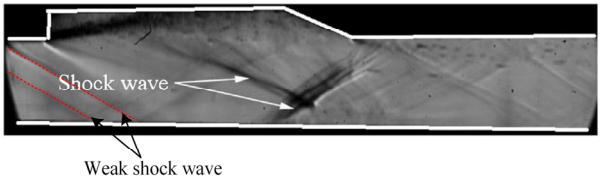

Fig. 3 High-speed Schlieren image of combustor without chemical reaction

3 Results and discussion

3.1 Wall pressure variation of different cases

Historical wall pressure variations of the monitor near the cavity ramp, obtained from different cases, are shown in Fig. 4. Black and blue solid lines represent the static pressures of case 1 and case 2, respectively. The experiment time sequences of kerosene and pilot H_2 are also added in Fig. 4. The red dotted and green dashed lines only express the times when valves open and close, not the real static pressure. As shown in Fig. 4, the pilot hydrogen is injected and ignited at t=1.880 s. During stage A, hydrogen is continually injected into the combustor. The wall pressure of the monitor starts to increase and reaches around 150 kPa. The pilot hydrogen is closed at t=2.220 s. From then on, there is no hydrogen in stage B. The liquid kerosene is injected at t=1.890 s and closed at t=2.500 s. It can be seen that the pilot hydrogen of different equivalence ratios in case 1 and case 2 is ignited by the spark plugs successfully.

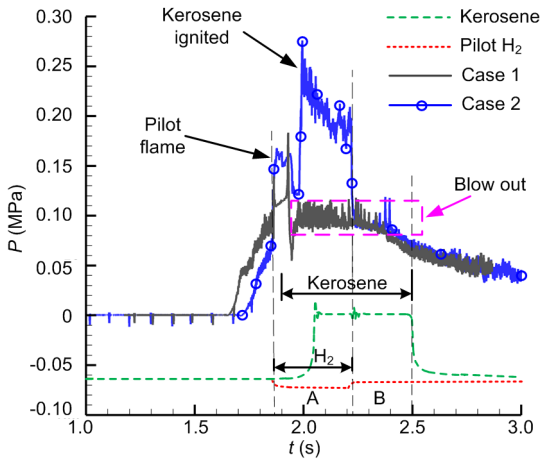

Fig. 4 Historical wall pressure (P) variations of pressure monitor in case 1 and case 2. References to color refer to the online version of this figure

In case 1, the wall pressure of the monitor suddenly collapses indicating the pilot flame is disabled

to ignite liquid kerosene and the pilot flame is blown out by kerosene of cold room temperature at around t=2.0 s. The flame, which is blown out, is marked with a pink dashed rectangle. Thus, the establishment of the kerosene flame fails. The average pressure distributions of different cases from t=2.100 s to t=2.200 s are displayed in Fig. 5. It is discovered that the pressure distribution of case 1 is slightly higher than that of case 3 which represents non-reacting flow.

In case 2, the wall pressure increases sharply and the maximal static pressure is around 0.28 MPa as shown in Fig. 4, meaning liquid kerosene is ignited by the pilot flame. The pressure distribution of case 2 is apparently higher than the others and the maximal static pressure is around 0.35 MPa as shown in Fig. 5. Simultaneously, the high back pressure induced by intense combustion spreads into the isolator and the most upstream position is x=0.15 m.

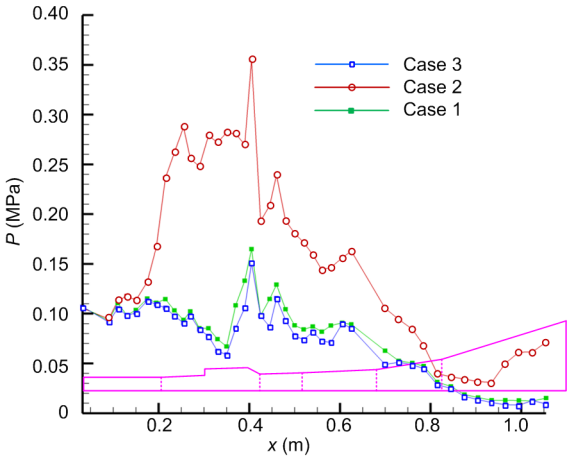

Fig. 5 Wall pressure distributions of three cases

By comparing the results of different cases, the successful ignition of kerosene can be achieved when the equivalence ratio of pilot hydrogen reaches 0.080. Therefore, larger heat release of pilot flame is beneficial to ignition. The type of fuel injection in stage A can evaluate the effects of hydrogen equivalence ratio on the establishment of the kerosene flame. At t=2.220 s, the wall pressure of the monitor in case 2 reduces to 0.09 MPa as soon as the injection of hydrogen stops. The phenomenon shows that the kerosene flame blows out without the injection of pilot hydrogen. Thus, the continuous supply of pilot hydrogen is the key factor for the stabilization of a steady global flame, which has been verified by the type of fuel injection in stage B.

3.2 Flame development of different cases

Flame luminosity images of different cases at specific times are taken from the view of the side wall as displayed in Figs. 6 and 7. These images have demonstrated flame development with various parameters governing fuel injection and are used to study the combustion characteristics.

As shown in Fig. 6, the pilot flame establishes and distributes in the whole cavity, and especially attaches to the top wall of the cavity at t=1.880 s. The color of pilot flame is yellow. At t=1.890 s, the kerosene starts to be injected and ignited by the pilot flame with the flame color transforming from yellow to white. As time passes, the region of kerosene flame shrinks continuously. The flame of white color mostly locates in the shear layer and boundary layer downstream of the cavity. At t=1.970 s, there exists only a

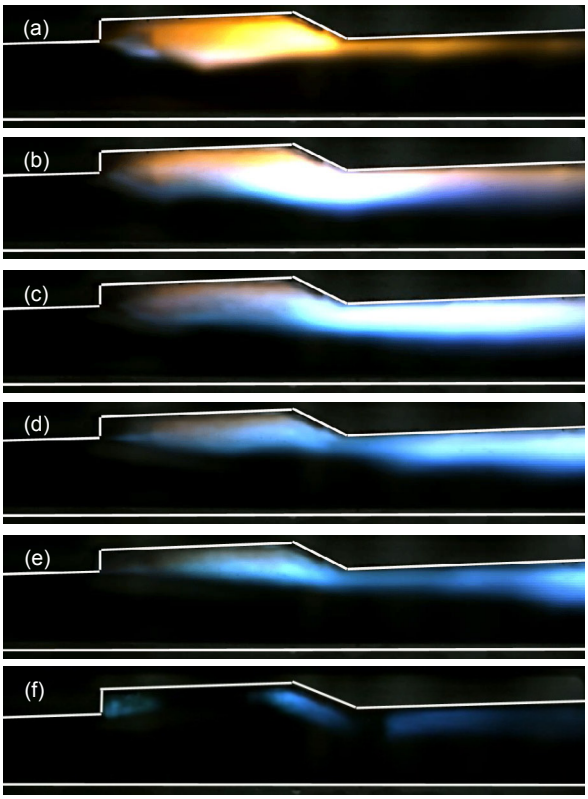

Fig. 6 Flame luminosity images of case 1 at different times (view from side wall)
(a) t=1.880 s; (b) t=1.890 s; (c) t=1.900 s; (d) t=1.910 s; (e) t=1.920 s; (f) t=1.970 s. References to color refer to the online version of this figure

very small region of flame anchored in the rear wall of the cavity. Finally, the pilot flame is blown out by liquid kerosene and the stabilization of the global flame fails.

With increased equivalence ratio of pilot hydrogen, the development of the flame shown in Fig. 7 is totally different from the above one. At t=1.970 s, the kerosene is ignited successfully. The flame fills the whole cavity and extends to the bottom wall of the combustor, and even spreads upstream of K1. Then, the flame undergoes a periodic variation as it propagates upstream and reduces repeatedly as illustrated from t=2.085 s to t=2.105 s. It is the larger heat release of pilot flame that leads to success in the establishment of combustion, nevertheless accompanied by oscillation.

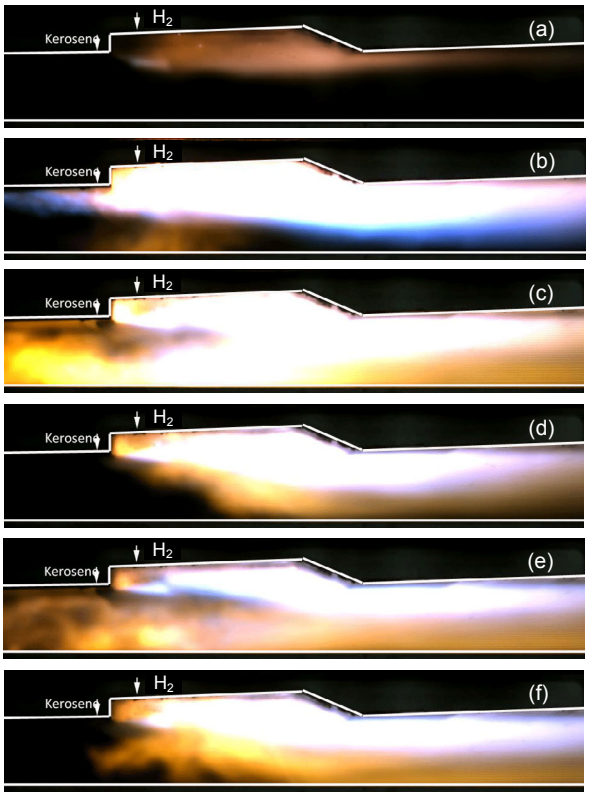

Fig. 7 Flame luminosity images of case 2 at different times (view from side wall)
(a) t=1.880 s; (b) t=1.970 s; (c) t=2.085 s; (d) t=2.090 s; (e) t=2.100 s; (f) t=2.105 s. References to color refer to the online version of this figure

In order to comprehend the 3D structures of the flame qualitatively, the flame luminosity images of cases 1 and 2 at different times viewed from the bottom wall are shown in Figs. 8 and 9, respectively. The direction of inflow is perpendicularly upward. Two spark plugs are located near the side walls of the combustor, which are used to ignite the pilot hydrogen.

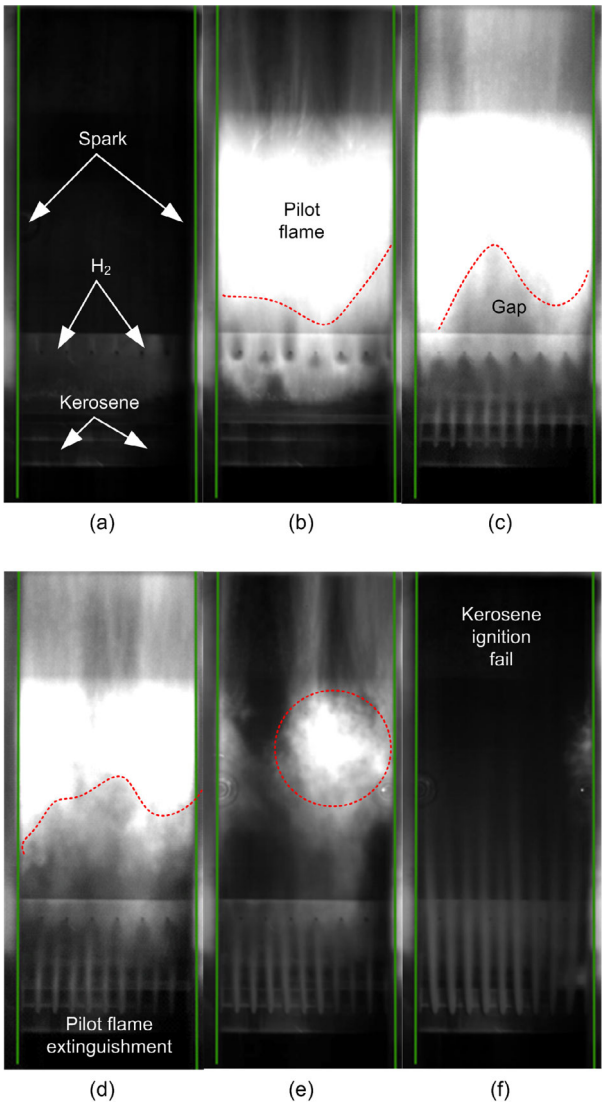

Fig. 8 Flame luminosity images of case 1 at different times (view from bottom wall)
(a) t=1.850 s; (b) t=1.880 s; (c) t=1.900 s; (d) t=1.905 s; (e) t=1.920 s; (f) t=1.970 s

Fig. 8 mainly presents the dynamic process of pilot flame extinguishment. As shown, the width of the combustor is filled with the pilot flame at t= 1.880 s and the leading edge of the flame reaches the

front step of the cavity. At t=1.890 s, liquid kerosene is injected perpendicularly into the main flow, and a flame gap appears in the middle of the combustor. The continuity of the pilot flame is broken and the gap grows. The flame viewed from the bottom wall is asymmetric. Then, the pilot flame around injection portholes nearly extinguishes and there is a small flame located at the cavity ramp. Finally, the pilot flame is blown out, failing to ignite the kerosene and establish a global flame.

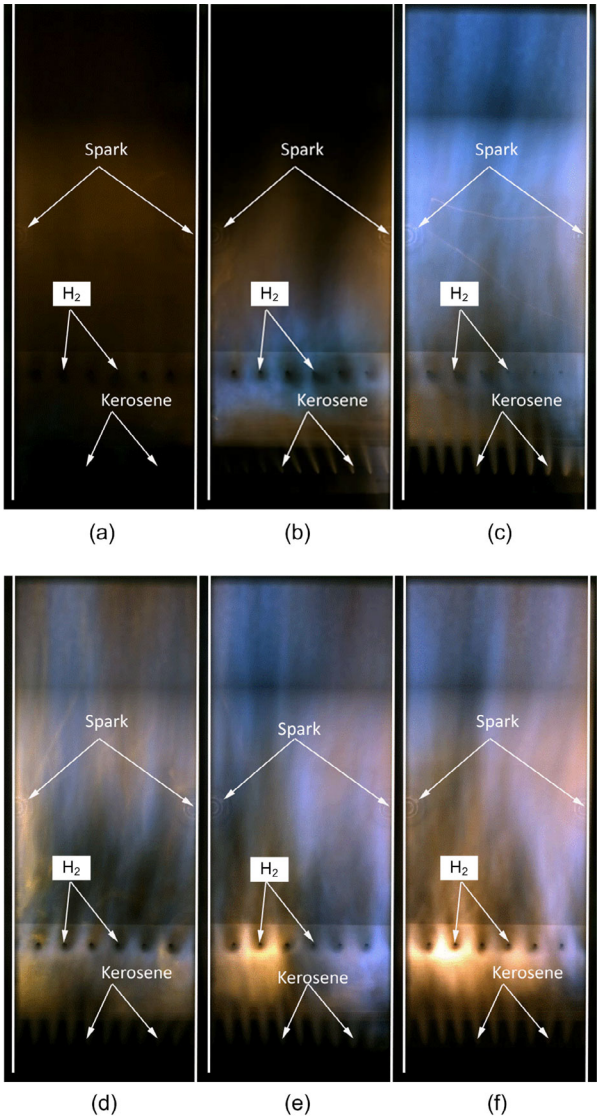

Fig. 9 Flame luminosity images of case 2 at different times (view from bottom wall)

(a) t=1.880 s; (b) t=1.970 s; (c) t=1.990 s; (d) t=2.000 s; (e) t=2.050 s; (f) t=2.100 s. References to color refer to the online version of this figure

In case 2, the liquid kerosene is ignited by the pilot flame, but the combustion is unstable. As shown in Fig. 9, the kerosene flame enlarges promptly from t=1.970 s to t=1.990 s. Especially, the injection direction of hydrogen affected by the thermal expansion is not perpendicular any more at t=1.970 s. The white flame, which fills the width of combustor, is also asymmetric. Then, the flame oscillates with repeated back and forth motions. For example, most of the white flame concentrates in the cavity and the leading edge locates upstream of the hydrogen injection portholes at t=2.050 s.

However, the white flame falls back downstream and the flame above the hydrogen injection portholes becomes yellow at t=2.100 s. Ignoring the pulsation of fuel mass flow rate and inflow, the flame oscillation results from complicated coupling between fluid and combustion. This study focuses on the process of flame stabilization but not the mechanism of flame oscillation. In order to obtain comprehensive understanding, more experiments should be carried out.

In order to distinguish the pilot and kerosene flames, the CH* luminosity images of case 2 are taken as shown in Figs. 10 and 11, where CH* is the intermediate product of fuel consumption, which is used to visualize the reaction zone. These images are viewed from the bottom wall and side wall, respectively. At different times, the kerosene mostly locates in the cavity shear layer, where the inflow, pilot hydrogen, and kerosene mix well, and attaches to the cavity ramp. Viewed from the bottom wall, the instability of the kerosene flame is remarkable as the region of kerosene chemical reaction demonstrates different shapes of crescent.

Concurrently, Schlieren images of inflow taken with a high-speed camera are shown in Fig. 12. The structures of shock waves and kerosene can be seen clearly. At t=1.880 s, the pilot flame stays in the cavity shear layer and the inflow is compressed from the cavity step. Thus, an oblique shock wave generates from the cavity step and attaches to the bottom wall of the combustor causing a small separation. At t=2.100 s and t=2.200 s, the thick black region represents non-reacting kerosene and the combustion of kerosene mostly occurs around the cavity ramp. When the injection of hydrogen stops, the kerosene flame is blown out at t=2.400 s. Without the pilot flame, the kerosene fills the whole cavity and locates

near the cavity bottom wall. Therefore, the unstable combustion is accompanied by various structural changes of shock waves.

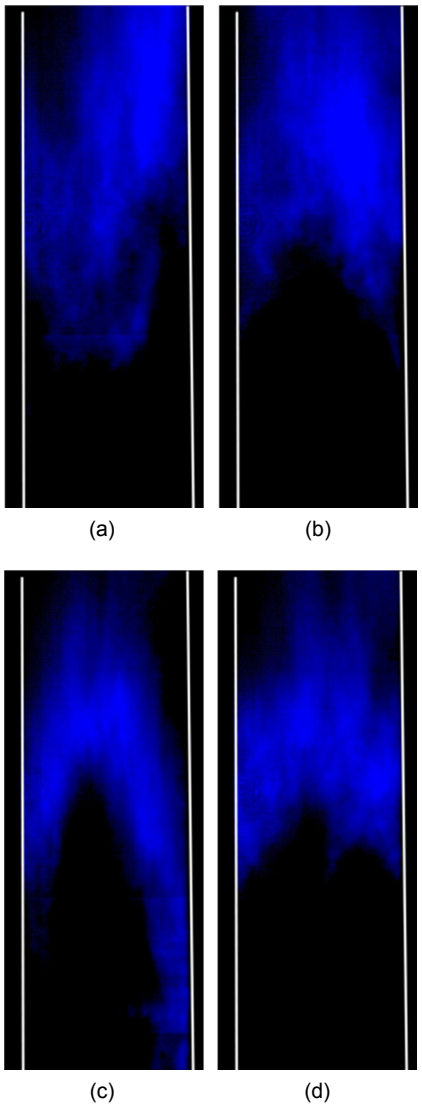

Fig. 10 CH* luminosity images of case 2 at different times (view from bottom wall)
(a) t=1.990 s; (b) t=2.000 s; (c) t=2.100 s; (d) t=2.200 s

4 Conclusions

Combustor characteristics in a kerosene-fueled scramjet combustor with a cavity of L/D=11.0 were imaged using Schlieren photography and flame luminosity, along with wall pressure measurements. The experiments were conducted in a direct-connected supersonic combustion facility with a

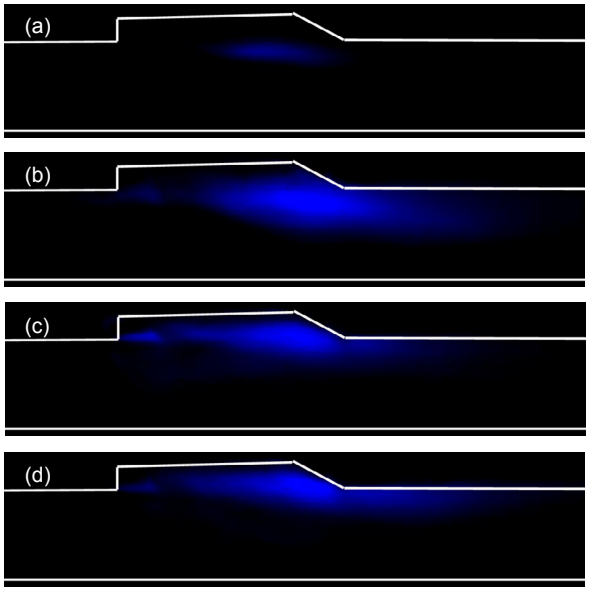

Fig. 11 CH* luminosity images of case 2 at different times (view from side wall)
(a) t=1.990 s; (b) t=2.000 s; (c) t=2.100 s; (d) t=2.200 s

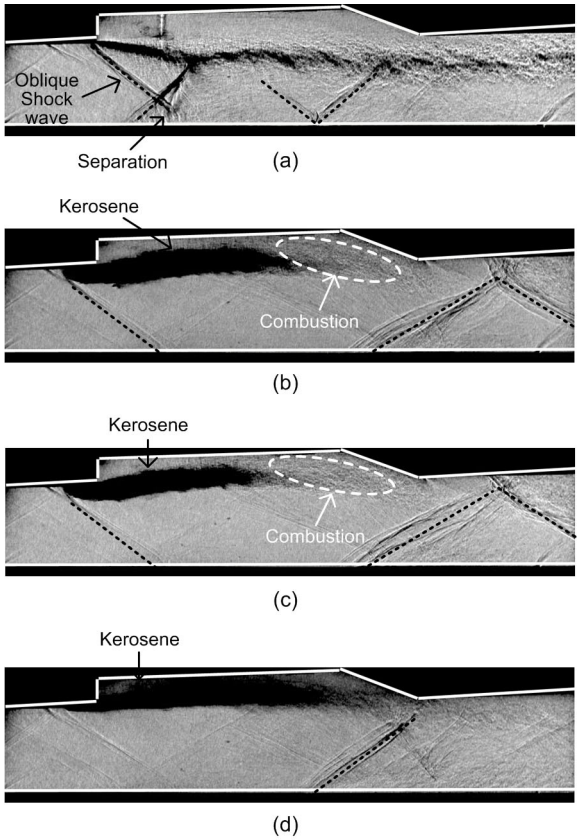

Fig. 12 Schlieren images of case 2 at different times (view from side wall)
(a) t=1.880 s; (b) t=2.100 s; (c) t=2.200 s; (d) t=2.400 s

stagnation temperature of 950 K and at a pressure of 0.82 MPa. The H_2/O_2 vitiated air heater provided high-enthalpy inflow of 2.68 kg/s, consisting of 21% O_2, 12% H_2O, and 67% N_2 in molar composition. Flight condition of Mach number 4.0 has been simulated. There are some meaningful observations in this study which are presented as follows:

1. Comparing wall pressure distributions of case 1 and case 2, it is found that the kerosene could be ignited when the equivalence ratio of pilot hydrogen was 0.080, rather than 0.040. In case 2, the high back pressure induced by intense kerosene combustion spread into the isolator and the leading edge of the shock train located at x=0.15 m.

2. Before the injection of kerosene, the pilot flame mostly located in the cavity shear layer and caused an oblique shock wave. This oblique shock wave was generated from the cavity step and attached to the bottom wall of the combustor, resulting in a new separation. Kerosene combustion generally occurred in the cavity shear layer. In case 2, the kerosene flame was asymmetrical and mainly attached to the cavity ramp. Meanwhile, combustion was unstable with repeated back and forth motions.

3. For this particular combustor, the pilot hydrogen of a certain equivalence ratio is a precondition for ignition. The evolution of flame stabilization and unstable combustion are obtained.

Since the stabilization and development of the flame are essential to the flight condition, background waves of isolator, geometry and location of the flameholder, and the strategy of fuel injection, further investigation should be carried out to gain comprehensive knowledge about ignition and blowout limits, region of equivalence ratio for stable combustion, and injection strategy for optimal scramjet performance.

Contributors

Ye TIAN and Jia-ling LE designed the research. Wen SHI and Fu-yu ZHONG processed the corresponding data. Ye TIAN wrote the first draft of the manuscript. Wan-zhou ZHANG and Wei-xin DENG helped to organize the manuscript. Wen SHI and Ye TIAN revised and edited the final version.

Conflict of interest

Wen SHI, Ye TIAN, Wan-zhou ZHANG, Wei-xin DENG, Fu-yu ZHONG, and Jia-ling LE declare that they have no conflict of interest.

References

Chang EWKC, Yang SM, Park G, et al., 2018. Ethylene flame-holding in double ramp flows. *Aerospace Science and Technology*, 80:413-423. https://doi.org/10.1016/j.ast.2018.07.012

Chang JT, Zhang JL, Bao W, et al., 2018. Research progress on strut-equipped supersonic combustors for scramjet application. *Progress in Aerospace Sciences*, 103:1-30. https://doi.org/10.1016/j.paerosci.2018.10.002

Feng R, Li J, Wu Y, et al., 2018. Experimental investigation on gliding arc discharge plasma ignition and flame stabilization in scramjet combustor. *Aerospace Science and Technology*, 79:145-153. https://doi.org/10.1016/j.ast.2018.05.036

Huang W, Yan L, 2013. Progress in research on mixing techniques for transverse injection flow fields in supersonic crossflows. *Journal of Zhejiang University-SCIENCE A (Applied Physics & Engineering)*, 14(8):554-564. https://doi.org/10.1631/jzus.A1300096

Huang W, Li MH, Ding F, et al., 2016. Supersonic mixing augmentation mechanism induced by a wall-mounted cavity configuration. *Journal of Zhejiang University-SCIENCE A (Applied Physics & Engineering)*, 17(1):45-53. https://doi.org/10.1631/jzus.A1500244

Kim K, Park G, Jin S, 2019. Flameholding characteristics of ethylene-fueled model scramjet in shock tunnel. *Acta Astronautica*, 161:446-464. https://doi.org/10.1016/j.actaastro.2019.02.022

Liao L, Yan L, Huang W, et al., 2018. Mode transition process in a typical strut-based scramjet combustor based on a parametric study. *Journal of Zhejiang University-SCIENCE A (Applied Physics & Engineering)*, 19(6):431-451. https://doi.org/10.1631/jzus.A1700617

Niioka T, Terada K, Kobayashi H, et al., 1995. Flame stabilization characteristics of strut divided into two parts in supersonic airflow. *Journal of Propulsion and Power*, 11(1):112-116. https://doi.org/10.2514/3.23847

Sun MB, Wang ZG, Liang JH, et al., 2008. Flame characteristics in supersonic combustor with hydrogen injection upstream of cavity flameholder. *Journal of Propulsion and Power*, 24(4):688-696. https://doi.org/10.2514/1.34970

Sun MB, Gong C, Zhang SP, et al., 2012. Spark ignition process in a scramjet combustor fueled by hydrogen and equipped with multi-cavities at Mach 4 flight condition. *Experimental Thermal and Fluid Science*, 43:90-96. https://doi.org/10.1016/j.expthermflusci.2012.03.028

Wang HB, Wang ZG, Sun MB, et al., 2013. Combustion modes of hydrogen jet combustion in a cavity-based supersonic combustor. *International Journal of Hydrogen Energy*, 38(27):12078-12089. https://doi.org/10.1016/j.ijhydene.2013.06.132

Wang YH, Song WY, 2019. Experimental investigation of influence factors on flame holding in a supersonic combustor. *Aerospace Science and Technology*, 85:180-186. https://doi.org/10.1016/j.ast.2018.12.002

Wang YH, Song YW, Fu Q, et al., 2017. Experimental study of vitiation effects on hydrogen/kerosene fueled supersonic combustor. *Aerospace Science and Technology*, 60:108-114. https://doi.org/10.1016/j.ast.2016.11.002

Wang ZG, Sun MB, Wang HB, et al., 2015. Mixing-related low frequency oscillation of combustion in an ethylene-fueled supersonic combustor. *Proceedings of the Combustion Institute*, 35(2):2137-2144. https://doi.org/10.1016/j.proci.2014.09.005

Zhang JL, Chang JT, Shi W, et al., 2018. Combustion stabilizations in a liquid kerosene fueled supersonic combustor equipped with an integrated pilot strut. *Aerospace Science and Technology*, 77:83-91. https://doi.org/10.1016/j.ast.2018.02.035

Zhang LW, Choi JY, Yang V, 2015. Supersonic combustion and flame stabilization of coflow ethylene and air with splitter plate. *Journal of Propulsion and Power*, 31(5):1242-1255. https://doi.org/10.2514/1.B35740

Zhao GY, Sun MB, Wu JS, et al., 2019. Investigation of flame flashback phenomenon in a supersonic crossflow with ethylene injection upstream of cavity flameholder. *Aerospace Science and Technology*, 87:190-206. https://doi.org/10.1016/j.ast.2019.02.018

Zhu SH, Xu X, Yang QC, et al., 2018. Intermittent back-flash phenomenon of supersonic combustion in the staged-strut scramjet engine. *Aerospace Science and Technology*, 79:70-74. https://doi.org/10.1016/j.ast.2018.05.037

中文概要

题　目： 先锋氢引燃煤油的超燃燃烧室火焰稳定性研究

目　的： 1. 在模拟飞行马赫数 4.0 条件下，通过直连实验研究先锋氢当量比对煤油燃料冲压发动机点火及稳焰的影响；2. 通过多种非接触光学测量手段研究超燃冲压发动机内燃烧流场的结构变化和火焰建立等动态过程。

创新点： 1. 通过直连实验发现，适量提高先锋氢当量比有利于发动机点火，且先锋氢的存在是发动机稳燃的前提；2. 得到了超燃发动机点火及燃烧不稳定特征的流场。

方　法： 1. 通过直连实验，得到监测点压力动态变化数据并对其进行分析（图 4 和 5）；2. 通过光学测量手段，观测流场及火焰动态变化过程（图 6~12）。

结　论： 1. 当先锋氢当量比为 0.080 时，煤油燃料超燃冲压发动机成功点火；当先锋氢当量比为 0.040 时，点火失败；当先锋氢关闭后，超燃冲压发动机熄火。2. 煤油火焰主要集中于凹槽后缘斜坡且结构是非对称的；燃烧是不稳定的且伴随着反复的前后移动。

关键词： 超燃冲压发动机；火焰稳定性；先锋氢；煤油；超声速燃烧